Fundamentals of Stable Continuum Generation at High Repetition Rates

Kohichi R. Tamura, *Member, IEEE*, Hirokazu Kubota, and Masataka Nakazawa, *Fellow, IEEE*

***Abstract*—A continuum generated from highly nonlinear seed pulses ($N \gg 1$) propagating in a medium with only self-phase modulation (SPM) or with SPM and anomalous dispersion is highly sensitive to the noise of the input pump pulse. The combination of SPM and normal dispersion improves the stability. However, more efficient spectral broadening schemes are desirable for generating a broad-band continuum at gigahertz rates. The adiabatic compression of weakly nonlinear pulses ($N \simeq 1$) via the soliton effect efficiently generates a broad-band continuum that is robust against noise. Detailed characterization of continuum generation in several different fibers is reported.**

***Index Terms*—Optical fiber devices, optical noise, optical propagation in dispersive media, optical propagation in nonlinear media, optical pulse compression, optical solitons.**

I. Introduction

CONTINUUM generation is an important method for obtaing broad optical spectra that can be spectrally sliced over a wide wavelength range [1]. In early work, it was generated using low-repetition-rate pump pulses from amplified femtosecond lasers and short lengths of fiber or bulk material. More recently, Morioka *et al.* showed that conceptually similar techniques can be implemented at gigahertz rates for use in optical communications [2]–[7]. The pump pulses are picoseconds in duration and the fibers are typically several hundreds of meters to kilometers in length. Their supercontinuum (SC) source has been used to demonstrate data transmission at rates of 1–3 Tb/s [8], [9]. Many variations on the SC source have since been reported [10]–[15].

The key to the SC source is a dispersion-flattened dispersion decreasing fiber (DDF), which generates a continuum that is extremely broad (over 200 nm), smooth (less than 10 dB of ripple), symmetric about the pump wavelength [6], [16], and stable against input pump noise [17]. The stability is especially important because even small amounts of noise at the input can translate into large fluctuations in the continuum [17]–[20]. Recent studies showed that adiabatic soliton compression can efficiently and stably broaden the spectrum in the presence of noise [18]–[20].

This paper summarizes fundamentals of stable spectral broadening in the presence of noise for the design of continuum light sources operating at gigahertz rates. The content elaborates on work reported in [18]–[20]. In Section II, the stabilities of four basic cases against noise are examined using a simple model. In Section III, several of the conclusions of Section II are verified experimentally. Section IV ends with the conclusion.

Manuscript received December 2, 1999; revised February 22, 2000.

The authors are with NTT Network Innovation Laboratories, Kanagawa 239-0847, Japan.

Publisher Item Identifier S 0018-9197(00)05443-9.

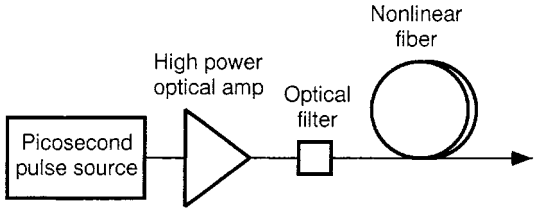

Fig. 1. Scheme for high-repetition-rate continuum generation.

II. Numerical Study of Continuum Generation

A. Numerical Model

Fig. 1 shows the system used for continuum generation. Picosecond pulses are amplified, filtered, and launched into a nonlinear fiber. The amplifier introduces amplified spontaneous emission (ASE) noise. An accurate model requires one to consider all of the nonlinear and higher order dispersive effects [1], [21]. However, at gigahertz rates, the peak powers are low (less than 10 kW); hence, most of the basic physics can be discerned by considering the effects of self-phase modulation (SPM) and second-order dispersion. Here, we choose to assume a linearly polarized pump pulse at a single wavelength, hence, cross-phase modulation (XPM) and effects of birefringence are neglected. These have been studied in detail elsewhere [1]. The propagation of a pulse with field a is then modeled by the nonlinear Schroedinger equation, which is given by

$$i\frac{da}{dz} = \frac{1}{2}\beta_2\frac{d^2a}{dt^2} - \gamma|a|^2a \tag{1}$$

where β_2 is the dispersion, $\gamma = 2\pi n_2/(\lambda A_{\text{eff}})$ is the nonlinear coefficient of the fiber, n_2 is the intensity-dependent index, λ is the wavelength, A_{eff} is the effective area, and $|a|^2$ is normalized to power.

For the initial field, we use $a_i(t) = a_o(t) + \Delta a(t)$, where $a_o = A_o \exp(-t^2/(2\tau^2))$. The pulse energy $E_a = \sqrt{\pi}|A_o|^2\tau$. $\tau_p = 2\sqrt{\ln 2}\tau$ is the pulse width at full-width at half-maximum (FWHM), and T is the width of the numerical calculation window. For simplicity, A_o is assumed to be real. $\Delta a(t)$ is the noise from the amplifier and is derived from a complex zero-mean white Gaussian process $n(t)$ with statistics given by $\langle n(t)\rangle = 0$, $\langle n(t)n(s)\rangle = 0$, and $\langle n(t)n^*(s)\rangle = (N_o/2)\delta(t-s)$ that are passed through a filter with a noise bandwidth B_f. The filter is assumed to have a Gaussian transmission characteristic

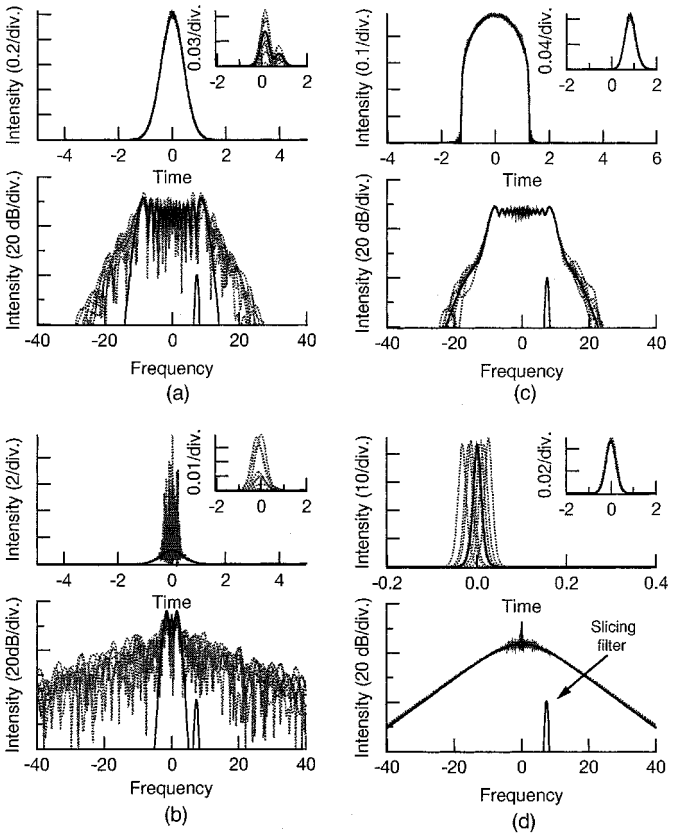

Fig. 2. Numerical results for continuum generation when $\sigma \simeq 30$ dB. (a) SPM only. (b) SPM and uniform anomalous dispersion. (c) SPM and uniform normal dispersion. (d) DDF. For each case: (top) continuum pulse, (top, inset) sliced pulse at $f = 7.4$, (bottom) spectra with slicing filter passband shown at $f = 7.4$. Solid traces correspond to noiseless cases. Dashed traces correspond to eight sample cases with random noise.

with $B_f \gg B_o$ where B_o is the bandwidth at FWHM of a_o. Although the average noise power at the filter output is $N_o B_f/2$, only the noise that temporally overlaps with the pulse affects the continuum. Hence, here we choose to define an effective amount of noise energy given by $E_n = N_o B_f \tau_p/2$, which corresponds to the noise gated by the pulsewidth. The effective signal-to-noise ratio σ at the fiber input is

$$\sigma = \frac{E_a}{E_n} = \sqrt{\frac{\pi}{\ln 2}} \frac{|A_o|^2}{B_f N_o}. \tag{2}$$

The nonlinear length $L_N = 1/(\gamma |A_o|^2)$, the dispersion length $L_D = \tau^2/(\beta_2)$, and $N^2 = L_D/L_N$.

To study the effects of noise, (1) was solved numerically using the split-step Fourier method for an initial condition a_i with $A_o = 1$, $\tau_p = 1$, and $B_f = 20 B_o$. The temporal window had a width of 10 τ_p and a grid of 4096 points. We chose four idealized cases for the nonlinear fiber: SPM only [Fig. 2(a)], SPM and uniform anomalous dispersion [Fig. 2(b)], SPM and uniform normal dispersion [Fig. 2(c)], and a DDF [Fig. 2(d)]. The fiber parameters were chosen to produce spectra of comparable root mean square (rms) spectral widths. The noise was fixed at $N_o/2 = 10^{-4}$, which gives $\sigma \sim 30$ dB. The results are summarized in Fig. 2, which shows the continuum pulse (upper traces), spectrum (lower traces), and the pulse obtained by slicing the continuum at $f = 7.4$ using a unit bandwidth Gaussian filter (inset traces). The pass band of the slicing filter is also shown in each spectrum, as indicated in the figure. Eight samples with random noise (dotted or dashed gray traces) and the noiseless case (dark solid trace) are overlaid in each figure. Each case is briefly discussed.

B. SPM with Infinite N

When $\beta_2 = 0$, a is given by

$$a = a_i \exp(-j\kappa |a_i|^2) = a_i \exp(-j\Phi) \tag{3}$$

where $\kappa = \gamma L_f$ and N is infinite. The nonlinear phase variation is given by $\Delta\Phi \equiv \kappa(|a + \Delta a|^2 - |a|^2)$, and its variance to first order in Δa is given by

$$\langle \Delta\Phi^2 \rangle_{\max} \simeq (\kappa a_i(0))^2 B_f N_o \simeq 2.1 \frac{\Phi_p^2}{\sigma} \tag{4}$$

where $\Phi_p = \kappa |A_o|^2$ and the filtered noise has been treated as approximately white. This expression gives a measure of the upper bound of the instantaneous fluctuations in the nonlinear phase. Stability of the continuum requires $\sqrt{\langle \Delta\Phi^2 \rangle_{\max}} \ll \pi$. Suppose $\Phi_p = 43$ which gives an rms spectral broadening by a factor of approximately 38. $\sqrt{\langle \Delta\Phi^2 \rangle_{\max}} < 0.1$ requires $\sigma > 56$ dB. Fig. 2(a) is the result for $\Phi_p = 43$. The phase variation $\sqrt{\langle \Delta\Phi^2 \rangle_{\max}} \simeq 1.2$ does not satisfy the stability condition, and the numerical results confirm the instability. The sliced pulse is temporally shifted due to the upchirp induced by SPM. The pulse shape is distorted because the SPM-induced chirp is nonlinear.

C. SPM and Uniform Dispersion with $N \gg 1$

The propagation of highly nonlinear pulses in a medium with SPM and uniform dispersion has been studied extensively [22]–[25]. Although the anomalous dispersion regime appears attractive because soliton compression can be exploited to enhance the nonlinear effects, the nonlinear pulse evolution is found to be unstable with respect to noise [18]–[20]. Fig. 2(b) shows the calculation results for $\gamma = 1$ ($L_N = 1$), $\beta_2 = -0.0002$ ($L_D \simeq 1.8 \times 10^3$), $N \simeq 42.5$, and $L_f = 9$. The spectrum in the noiseless case has hardly broadened; however, noise spikes are rapidly enhanced by the modulational instability (MI) effect [21]. MI occurs when the interplay of SPM and anomalous dispersion enhances small perturbations. The signature of MI in the spectrum is spectral side lobes [21]. The growth rate of noise spikes associated with MI can be shown to be faster than the spectral broadening rate of the main pulse. Following the work in pulse compressors, the pulse compression factor F_c and the optimal fiber length L_{opt} are approximated by the following empirical expressions when $N \gg 1$ and the input pulse is a hyperbolic secant shape [21]

$$F_c = 4.1N \tag{5}$$

$$\begin{aligned} L_{\text{opt}} &= \left(\frac{0.32}{N} + \frac{1.1}{N^2} \right) \frac{\pi}{2} L_D \\ &= \frac{\pi}{2} (0.32 \sqrt{L_D L_N} + 1.1 L_N) \end{aligned} \tag{6}$$

where $L_{\rm opt}$ is the length at which the energy in the compressed pulse is maximized and the pedestal energy is minimized. The characteristic length $L_{\rm MI}$ associated with the peak MI gain at the pulse peak is given by

$$L_{\rm MI} \simeq \frac{1}{2\gamma|A_o|^2} = \frac{1}{2}L_N. \tag{7}$$

$L_D \gg L_N$, therefore $L_{\rm MI} < L_{\rm opt}$. One may conclude that the instability of higher order solitons in the presence of noise makes them unsuitable for stable continuum generation [19].

There is a significant difference if the dispersion is normal [19], [20]. The instability due to noise is greatly reduced because, not only does MI not occur, the normal dispersion smoothes the noise perturbations. Fig. 2(c) shows the calculation results for $\gamma = 1$ ($L_N = 1$), $\beta_2 = +0.0002$ ($L_D \simeq 1.8 \times 10^3$), $N \simeq 42.5$, and $L_f = 60$. The pulse evolves into the well-known linearly chirped square pulse with rapid oscillations at the pulse edges due to optical wave breaking [24]. Optical wave breaking occurs when frequency components in the central portion of the pulse overtake and interfere with slower traveling components at the pulse wings. This pulse is stable against noise.

These results suggest that continuum generation in a normally dispersive fiber is an attractive approach. However, practical difficulties arise when operating at gigahertz rates. Consider the generation of a continuum with a spectral broadening factor of ~100. Again, following work in pulse compressors that operate in the normal dispersion regime (fiber/grating compressors), F_c is given by

$$F_c \simeq \frac{N}{k}. \tag{8}$$

$F_c \sim 100$ should give a spectral broadening of the same order. k depends on the initial pulse shape. Using $k = 1.6$, which is appropriate for sech input pulses, one finds that $N > 600$ is necessary. In comparison, only $N > 24$ is necessary when exploiting higher order soliton effects [see (5)]. Next, consider the generation of $N = 600$ pulses in a fiber with a mode field diameter of 4.2 μm using seed pulses with an average power of 100 mW, a pulsewidth of 3.5 ps, and a pulse period of 100 ps. When the dispersion is zero, a 4.2-km length of fiber is required to obtain an rms spectral broadening of 100. An even longer fiber is needed if normal dispersion is introduced. An $N = 600$ input pulse requires $\beta_2 < 4 \times 10^{-4}$ ps^2/km. At such low dispersion values, the dispersion slope becomes significant [26]–[28]. Beyond the zero dispersion wavelength, the continuum is unstable due to MI. Since the long- and short-wavelength regimes temporally overlap, the entire spectrum becomes unstable. Dispersion-flattened fibers (DFF's) may be used to solve the problem of dispersion slope. A recent experiment performed at 10 GHz in a DFF with a dispersion of -0.1 ps/nm/km and a length of 1720 m produced a spectrum with a -10-dB bandwidth of 20.9 nm [14]. Obtaining broader bandwidths with this approach will require very high energy pump pulses.

D. SPM and Decreasing Anomalous Dispersion with $N \simeq 1$

A DDF is a fiber with an anomalous dispersion that decreases in magnitude with length [29]–[31]. Its effectiveness for generating a stable continuum has been demonstrated [17]–[20]. If the taper is sufficiently slow and the input pulse is approximately an $N = 1$ soliton, the soliton adiabatically compresses [32] to maintain the soliton area theorem [33], [34]. This theorem predicts that the compression factor is proportional to the ratio of input-to-output dispersion, which ideally results in infinite compression if the dispersion tapers to zero. In actuality, higher order dispersive effects limit the bandwidth. Nevertheless, a broad continuum can be generated efficiently because the peak power increases as the pulse is compressed. The continuum is also robust against noise because, to first order, the noise only perturbs the center frequency of the soliton. This frequency shift translates into timing jitter (known as Gordon–Haus jitter) via the dispersion [35]–[37].

Fig. 2(d) shows the calculation results with a DDF. The dispersion was assumed to have an exponentially decreasing profile given by $\beta_2(z) = \beta_o \exp(-z/z_m)$ for $0 \le z \le L_f$. The calculation parameters were $z_m = 5$, $L_f = 20$, $\gamma = 1$, and $\beta_o = -\gamma/3.11$. The pulse compression factor at the output is approximately 50. Fig. 2(d) confirms that the effect of noise is predominantly to temporally displace the soliton, i.e., to introduce Gordon–Haus jitter. The stability of the spectrum is apparent.

TABLE I
EXPERIMENTAL PARAMETERS

Fiber	Length (km)	D (ps/nm/km)	D slope (ps/nm^2/km)	P_{in} (mW)	N_{in}	Continuum $\Delta\lambda$ (nm)
HNL-DSF1	1.0	-0.04	+0.033	100	19.3	17
HNL-DSF2	1.0	+0.10	+0.033	70	9.9	60
DFF	2.0	+0.32	+0.004	88	4.7	174
DDF	0.9	In +10 Out ≈0	+0.049	80	0.7	79

III. EXPERIMENTAL STUDY OF CONTINUUM GENERATION

To verify some of the conclusions of the previous section, continuum generation was experimentally studied using seed pulses at $\lambda_s = 1540.5$ nm from a regeneratively mode-locked fiber laser [38], [39] which had a repetition rate of ~10 GHz, a pulsewidth of 3.5 ps, a spectral width of 0.69 nm, and a time–bandwidth product of 0.30. The seed pulses were amplified in a high-power erbium–ytterbium-doped fiber amplifer. The output of the amplifier was filtered with a 10-nm bandwidth filter centered at 1540.5 nm. The filter broadened the pulsewidth to 3.9 ps.

The fibers that were used for continuum generation are summarized in Table I. Two were high nonlinearity dispersion-shifted fibers (HNL-DSF1, HNL-DSF2), which had mode field diameters of 4.2 μm. HNL-DSF1 and HNL-DSF2 had zero dispersion wavelengths λ_0 of 1544 nm and 1538 nm, respectively, and allowed for a comparison of launching in the normal and anomalous dispersion regimes. A DFF was chosen to examine the role of dispersion slope in the spectral broadening. The dispersion flattening was achieved by using a W-shaped core [40], resulting in an anomalous dispersion of less than 0.32 ps/nm/km between 1510 and 1598 nm. The last fiber was a DDF drawn from a step-index fiber preform,

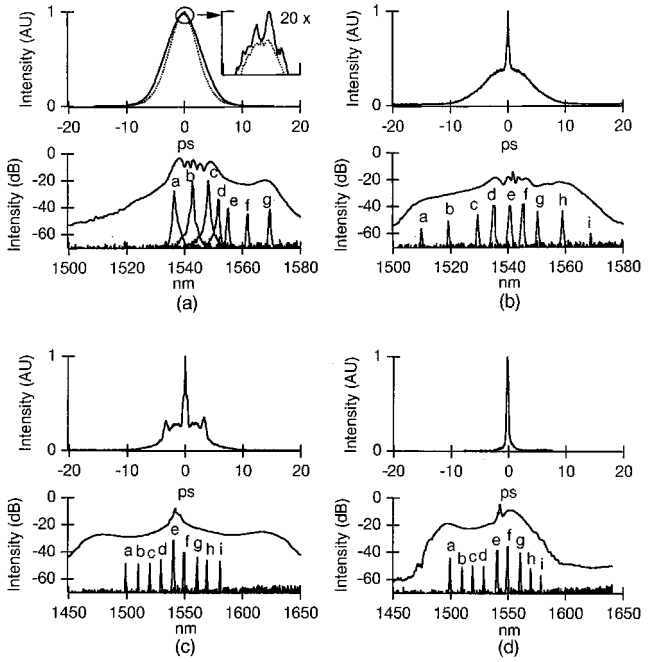

Fig. 3. Experimentally measured continuum spectra (lower traces) and background-free autocorrelations (upper traces) from: (a) HNL-DSF1, (b) HNL-DSF2, (c) DFF, and (d) DDF. Slices in the spectra are shown at high resolution in Fig. 6.

in which the drawing speed was changed to vary the core geometry and hence the local value of dispersion [30].

A. Spectral Broadening

First, the spectral broadening characteristics for the various fibers are compared. The input pulse conditions are listed in Table I, and the measured spectra are shown in Fig. 3. The slices correspond to locations at which the spectra were measured at high resolution using a scanning Fabry–Perot spectrometer. The corresponding Fabry–Perot spectra are shown in Fig. 6 and will be discussed in Section III-C. The spectral width of the continuum was narrowest for HNL-DSF1, even though N_i was highest [Fig. 3(a)]. The limited broadening reflects the reduced nonlinear efficiency of the normal dispersion regime. Equation (8) predicts a broadening by approximately 13, but the actual value is 24. The difference occurs because consideration of F_c alone ignores the efficiency of compression. The ratio of temporal compression to spectral broadening is typically less than 1:1. Fig. 3(b) shows the continuum from HNL-DSF2. The increased efficiency in the anomalous dispersion regime is evident from the difference in spectral width in comparison to HNL-DSF1. Fig. 3(c) is the continuum from the DFF and shows the role of dispersion slope in the spectral broadening. A dramatic increase in bandwidth is obtained in comparison to HNL-DSF2.

Fig. 3(d) is the continuum from the DDF. The efficient pulse compression leads to a broader spectrum than in the case of HNL-DSF2. However, due to the third-order dispersion, the spectrum is not as wide as that from the DFF. The spectral asymmetry that results is typical of what is observed when the effects of third-order dispersion are significant [31]. In particular, the longer wavelength side develops into a soliton-like

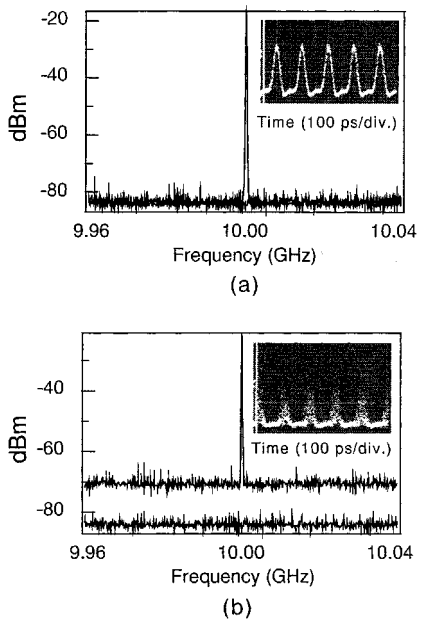

Fig. 4. RF spectrum and sampling oscilloscope trace (inset) of a 0.35-nm bandwidth spectrally sliced pulse at 1553.5 nm for (a) DDF and (b) HNL-DSF2.

spectrum with decaying wings, while the shorter wavelength side develops into a broad flat spectrum. Such spectral asymmetry is undesirable in applications such as pulse compression and can be reduced by using DFF's [41]. Each of the spectra shown in Fig. 3 exhibited long-term stability when viewed on a grating-scanned optical spectrum analyzer.

B. Pulse-to-Pulse Stability

HNL-DSF2 and the DFF correspond to the cases of SPM with uniform anomalous dispersion. From (6) and (7), $L_{\rm opt}$ and $L_{\rm MI}$ are 4.1 and 0.6 km, respectively, for HNL-DSF2 and 3.5 and 0.9 km, respectively, for the DFF. $L_{\rm MI} < L_{\rm opt}$, hence the continuum pulse should evolve into a noise burst. Noise bursts have autocorrelation profiles which have a coherence spike at zero time delay. The width of the coherence spike is inversely proportional to the bandwidth of the fluctuations. The contrast ratio, which is defined as the ratio of the peak of the autocorrelation to the peak neglecting the coherence spike, gives a measure of the degree of randomness.

Background-free autocorrelation measurements of the continuum pulses are also shown in Fig. 3 (upper traces). Coherence spikes can be seen in Fig. 3(a)–(c). The contrast ratios in Fig. 3(b) and (c) are close to 2:1, which are consistent with bursts of random noise. In Fig. 3(a), the contrast ratio is nearly unity, which indicates that the fluctuations are small. The random portion in this case may be attributed to the broad spectral tail in Fig. 3(a) (lower trace), which extends into the anomalous dispersion regime and experiences MI. Further support of this claim is given in the following section. Finally, Fig. 3(d) is the case of the DDF. The autocorrelation has a width of 300 fs and indicates a clean short pulse.

To further examine the pulse-to-pulse stability, the continuum from each fiber was sliced with a narrow-band filter, detected with a fast photodiode, and observed on a sampling oscilloscope and an RF spectrum analyzer. Fig. 4 compares the pulse trains

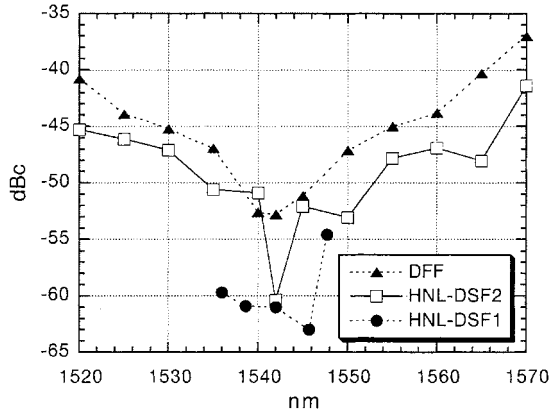

Fig. 5. White noise level versus wavelength as measured through a 1-nm bandwidth filter for HNL-DSF1, HNL-DSF2, and DFF. Noise is referenced to the carrier peak (dBc-dB below peak). The noise level was not observable for DDF.

obtained from the DDF and from HNL-DSF2 by slicing the continuum with a 0.35-nm bandwidth filter centered at 1553.5 nm. A stable 10-GHz pulse train was obtained for the DDF; however, the pulse train from HNL-DSF2 appeared random. The fluctuations appeared in the RF spectrum as a white noise floor well above the instrument measurement limit (flat level). The floor was not observable for the DDF. The sliced pulse train resulting from the DFF was similar to Fig. 4(b). The continuum from HNL-DSF1 had insufficient spectral energy at 1553.5 nm to be characterized.

The wavelength dependence of the white noise level as observed through a tunable 1-nm filter was measured. The results are shown in Fig. 5. The white noise floor, which was measured from the peak of the 10-GHz carrier, is lowest in the vicinity of λ_s and increases with increasing wavelength separation from λ_s. The white noise level was lower than the instrument limit for the DDF. The instability of HNL-DSF2 and the DFF in comparison to HNL-DSF1 and the DDF is apparent.

C. Optical Phase Coherence

The spectrum of the seed source was phase coherent, i.e., its spectrum consisted of a comb of frequencies with a $\sim$10-GHz spacing. The linewidth of a single optical mode has been measured to be less than 1 kHz [42]. The preservation of the frequency comb in the continuum is interesting for applications such as multiwavelength CW light generation. If the seed source consists of a comb of zero linewidth optical frequencies spaced by an even frequency interval, then this same optical comb structure should be preserved across the continuum if perfect mixing occurs. In the time domain, this is equivalent to the relative optical phases from pulse-to-pulse being preserved during the continuum generation. The development of random phase and/or amplitude jitter appears as a white incoherent spectral component.

To examine the preservation of the frequency comb within the continuum, high-resolution spectral measurements were made using a scanning Fabry–Perot spectrometer which had a finesse of $>$100, a free spectral range of $>$150 GHz, and a scanning rate of 20 ms. Aliasing in the Fabry–Perot was avoided by slicing the

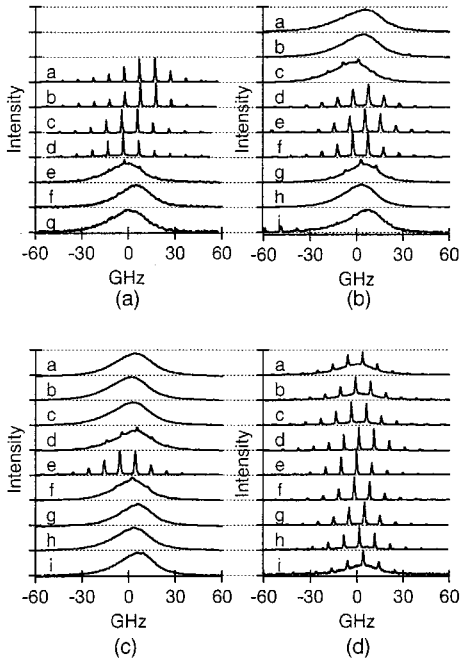

Fig. 6. High-resolution measurement of a sliced continuum for (a) HNL-DSF1, (b) HNL-DSF2, (c) DFF, and (d) DDF. The labels correspond to the spectral slices in Fig. 3.

continuum with a 0.2-nm bandwidth filter before measuring the spectrum at high resolution with the Fabry–Perot. Each spectral slice was measured by averaging on a digital oscilloscope over several minutes. The slices are shown in Fig. 3 and the corresponding spectra at high resolution are shown in Fig. 6. One finds that the discrete optical lines are preserved in large part across the spectrum from the DDF, which is another confirmation of its temporal stability [Fig. 6(d)]. The main portion of the continuum from HNL-DSF1 also shows phase coherency [Fig. 6(a)]. However, the tail in the anomalous dispersion regime shows no sign of discrete modes. These spectral regions most likely correspond to the small coherence spike in the autocorrelation of Fig. 3(a), which reflects the onset of MI. The initial pulse is launched in the normal dispersion regime; however, due to the dispersion slope, the long-wavelength side of the spectrum broadens into the anomalous dispersion regime. Here, MI occurs and begins to destabilize the spectrum. With further propagation, the entire spectrum will become unstable because the components that are made unstable by MI temporally overlap with the portion in the normal dispersion regime. The continuum from HNL-DSF2 and the DFF show phase coherence only in the region of λ_s.

The spectral stability of the DDF at low and high σ was confirmed by observing the stability of the sliced spectrum. σ was varied by changing the input power to the high-power amplifier and adjusting the amplifier gain to maintain a similar compressed pulse spectrum. If the compressed pulse spectrum is constant, then one may assume that the compression dynamics are the same and only σ has changed. σ was estimated from the input spectrum over a 4.2-nm range centered at 1540.5 nm. Fig. 7(a) shows a 1-nm spectral slice at 1567 nm from the DDF at $\sigma > 30$ dB, DDF at $\sigma \sim 23$ dB, and HNL-DSF2 at $\sigma >$ 30 dB. The slice from the DDF at high σ shows phase coherence,

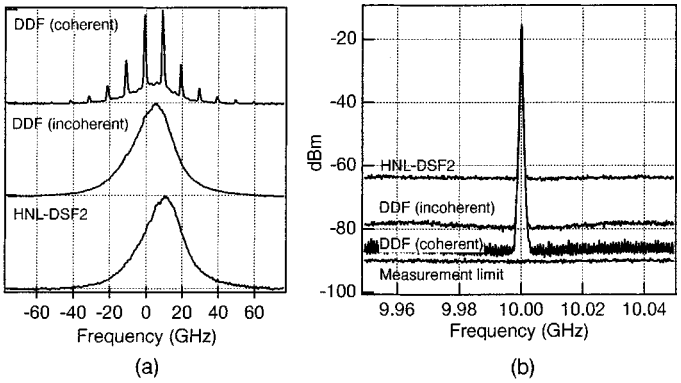

Fig. 7. Comparison of the stability of the pulse trains obtained with 1-nm bandwidth slicing filter at 1567 nm. (a) Optical spectra from DDF (coherent case), DDF (incoherent case), and HNL-DSF2. (b) RF spectra corresponding to optical spectra in (a).

but the other two cases show no phase coherence. Fig. 7(b) compares the RF spectra of each pulse train. The incoherent pulse train from the DDF at low σ has a white noise level that is degraded by 8–10 dB compared to the level at high σ. However, it is still lower by over 15 dB compared to HNL-DSF2, which attests to its stability.

D. Discussion

The experimental results support several of the predictions of Section II. First, the low efficiency of continuum generation in the normal dispersion regime is evident. Second, higher order solitons were shown to be unstable with respect to noise due to the onset of MI. Third, stable and relatively broad bandwidth spectra are obtained when using a DDF. However, low third-order dispersion is also necessary for generating extremely broad spectra which are symmetric. These considerations explain the success of the SC fiber, which broadens the spectrum of the pump pulse in a DDF with low third-order dispersion which tapers into the normal dispersion regime at the output end [17]. A variation on the SC fiber is to cascade a standard DDF with a normal dispersion fiber [12], [13]. This method raises the peak power and bandwidth of the pump pulse in the DDF and generates a broad flat spectrum in the normal dispersion fiber. It avoids the need for a dispersion-flattened DDF, which is a special fiber that is not readily available at the present time.

IV. Conclusions

This paper has reported numerical and experimental studies of several basic fiber designs for the generation of a stable continuum at high repetition rates. Continuum generation with highly nonlinear $(N \gg 1)$ pulses in a medium with SPM or with SPM and anomalous dispersion is highly sensitive to noise. The noise sensitivity is greatly reduced when using pulses with $N \gg 1$ in the normal dispersion regime. However, this approach has practical difficulties at high repetition rates because the spectral broadening has low efficiency. A DDF achieves efficient spectral broadening that is stable in the presence of noise. However, low third-order dispersion is necessary to obtain extremely broad bandwidths. The success of the remarkable SC fiber [4], [6] may be attributed to the fact that it broadens the spectrum of the pump pulse in a DDF that has very low third-order dispersion.

Acknowledgment

The authors would like to thank K. Mori for discussions on the SC source.

References

[1] R. R. Alfano, *The Supercontinuum Laser Source*. Berlin, Germany: Springer-Verlag, 1989.
[2] K. Mori, T. Morioka, H. Takara, and M. Saruwatari, "Continuum tunable optical pulse generation untilizing supercontinuum in an optical fiber pumped by amplified gain-switched LD pulses," in *Proc. Optical Amplifiers and Their Applications OA&A'93*, 1993, pp. 190–193.
[3] K. Morioka, K. Mori, S. Kawanishi, and M. Saruwatari, "Pulse-width tunable, self-frequency conversion of short optical pulses over 200 nm based on supercontinuum generation," *Electron. Lett.*, vol. 30, pp. 1960–1962, Nov. 1992.
[4] T. Morioka, S. Kawanishi, K. Mori, and M. Saruwatari, "Transform-limited, femtosecond WDM pulse generation by spectral filtering of GHz supercontinuum," *Electron. Lett.*, vol. 30, pp. 1166–1168, 1994.
[5] K. Morioka, K. Uchiyama, S. Kawanishi, M. Suzuki, and S. Saruwatari, "Multiwavelength picosecond pulse source with low jitter and high optical frequency stability based on 200 nm supercontinuum filtering," *Electron. Lett.*, vol. 31, pp. 1064–1066, June 1995.
[6] K. Mori, H. Takara, S. Kawanishi, M. Saruwatari, and T. Morioka, "Flatly broadened supercontinuum spectrum generated in a dispersion decreasing fiber with convex dispersion profile," *Electron. Lett.*, vol. 33, pp. 1806–1808, Oct. 1997.
[7] S. Kawanishi, K. Uchiyama, H. Takara, T. Morioka, M. Yamada, and T. Kanamori, "Nearly transform-limited 1.4 μm picosecond pulse generation by supercontinuum and pulse amplification in Tm-doped optical amplifier," *Electron. Lett.*, vol. 33, pp. 1553–1554, Aug. 1997.
[8] T. Morioka, H. Takara, S. Kawanishi, O. Kamatani, K. Takiguchi, K. Uchiyama, M. Saruwatari, H. Takahashi, M. Yamada, T. Kanamori, and H. Ono, "1 Tbit/s (100 Gbit/s $\times$ 10 channel) OTDM/WDM transmission using a single supercontinuum WDM source," *Electron. Lett.*, vol. 32, pp. 906–907, May 1996.
[9] S. Kawanishi, H. Takara, K. Uchiyama, I. Shake, and K. Mori, "3 Tbit/s (160 Gbit/s $\times$ 19 ch) OTDM/WDM transmission experiment," in *OFC/IOOC 1999 Postdeadline Papers*. paper PD1.
[10] K. Tamura, E. Yoshida, and M. Nakazawa, "Generation of 10 GHz pulse trains at 16 wavelengths by spectrally slicing a high power femtosecond source," *Electron. Lett.*, vol. 32, pp. 1961–1962, Aug. 1996.
[11] M. J. Guy, S. V. Chernikov, and J. R. Taylor, "Duration-tunable, multiwavelength pulse source for OTDM and WDM communications systems," *IEEE Photon. Technol. Lett.*, vol. 9, pp. 1017–1019, July 1997.
[12] H. Sotobayashi and K. Kitayama, "325 nm bandwidth supercontinuum generation at 10 Gbit/s using dispersion-flattened and nondecreasing normal dispersion fiber with pulse compression technique," *Electron. Lett.*, vol. 34, pp. 1336–1337, June 1998.
[13] Y. Takushima, F. Futami, and K. Kikuchi, "Generation of over 140-nm-wide super-continuum from a normal dispersion fiber by using a mode-locked semiconductor laser source," *IEEE Photon. Technol. Lett.*, vol. 10, pp. 1560–1562, Nov. 1998.
[14] Y. Takushima and K. Kikuchi, "10-GHz, over 20-channel multiwavelength pulse source by slicing super-continuum generated in normal-dispersion fiber," *IEEE Photon. Technol. Lett.*, vol. 11, pp. 322–324, Mar. 1999.
[15] B. Mikulla, L. Leng, S. Sears, B. C. Collings, M. Arend, and K. Bergman, "Broad-band high-repetition-rate source for spectrally sliced WDM," *IEEE Photon. Technol. Lett.*, vol. 11, pp. 418–420, Apr. 1999.
[16] T. Okuno, M. Onishi, and M. Nishimura, "Generation of ultra-broad-band supercontinuum by dispersion-flattened and decreasing fiber," *IEEE Photon. Technol. Lett.*, vol. 10, pp. 72–74, Jan. 1998.
[17] K. Mori, K. Takara, and S. Kawanishi, "The effect of pump fluctuation in supercontinuum pulse generation," *Nonlinear Guided Waves & Their Applications,OSA Tech. Dig. Ser.*, vol. 5, pp. 276–278, 1998. .
[18] M. Nakazawa, K. Tamura, H. Kubota, and E. Yoshida, "Coherence degradation in the process of supercontinuum generation in an optical fiber," *Opt. Fiber Technol.*, vol. 4, pp. 215–223, 1998.

[19] M. Nakazawa, H. Kubota, and K. Tamura, "Random evolution of high order optical solitons under the presence of amplified spontaneous emission," *Opt. Lett.*, vol. 25, pp. 318–320, Mar. 1999.
[20] H. Kubota, K. Tamura, and M. Nakazawa, "Analyzes of coherence-maintained ultrashort optical pulse trains and supercontinuum in the presence of soliton-amplified spontaneous-emission interaction," *J. Opt. Soc. Amer. B.*, vol. 16, pp. 2223–2232, Dec. 1999.
[21] G. P. Agrawal, *Nonlinear Fiber Optics*. New York, NY: Academic, 1989.
[22] L. F. Mollenauer, R. H. Stolen, J. P. Gordon, and W. J. Tomlinson, "Extreme picosecond pulse-narrowing by means of soliton effect in single-mode optical fibers," *Opt. Lett.*, vol. 8, pp. 289–291, May 1983.
[23] D. Grischkowsky and A. C. Balant, "Optical pulse compression based on enhanced frequency chirping," *Appl. Phys. Lett.*, vol. 41, July 1982.
[24] W. J. Tomlinson, R. J. Stolen, and C. V. Shank, "Compression of optical pulses chirped by self-phase modulation in fibers," *J. Opt. Soc. Amer. B.*, vol. 1, pp. 139–149, Apr. 1984.
[25] M. Nakazawa, K. Suzuki, H. Kubota, and H. A. Haus, "High-order solitons and the modulational instability," *Phys. Rev. A.*, vol. 39, pp. 5768–5776, June 1989.
[26] G. P. Agrawal and M. J. Potasek, "Nonlinear pulse distortion in single-mode optical fibers at the zero-dispersion wavelength," *Phys. Rev. A.*, vol. 33, pp. 1765–1776, Mar. 1986.
[27] P. K. A. Wai, C. R. Menyuk, Y. C. Lee, and H. H. Chen, "Nonlinear pulse propagation in the neighborhood of the zero-dispersion wavelength of monomode optical fibers," *Opt. Lett.*, vol. 11, pp. 464–466, July 1986.
[28] P. Beaud, W. Hodel, B. Zysset, and H. P. Weber, "Ultrashort pulse propagation, pulse breakup, and fundamental soliton formation in a single-mode optical fiber," *IEEE J. Quantum Electron.*, vol. 23, pp. 1938–1946, Nov. 1987.
[29] E. M. Dianov, P. V. Mamyshev, A. M. Prokhorov, and S. V. Chernikov, "Generation of a train of fundamental solitons at a high repetition rate in optical fibers," *Opt. Lett.*, vol. 14, pp. 1008–1010, Sept. 1989.
[30] V. A. Bogatyrev, M. M. Bubnov, E. M. Dianov, A. S. Kurkov, P. V. Mamyshev, A. M. Prokhorov, S. D. Rumyantsev, V. A. Semenov, S. L. Semenov, A. A. Sysoliatin, S. V. Chernikov, A. N. Gur'yanov, G. G. Devyatykh, and S. I. Miroshnichenko, "A single mode fiber with chromatic dispersion varying along the length," *J. Lightwave Technol.*, vol. 9, pp. 561–566, May 1991.
[31] S. V. Chernikov, D. J. Richardson, E. M. Dianov, and D. N. Payne, "Picosecond soliton pulse compressor based on dispersion decreasing fiber," *Electron. Lett.*, vol. 28, pp. 1842–1844, 1992.
[32] K. J. Blow, N. J. Doran, and D. Wood, "Generation and stabilization of short soliton pulses in the amplified nonlinear Schroedinger equation," *J. Opt. Soc. Amer. B*, vol. 5, pp. 381–390, Feb. 1988.
[33] V. E. Zakharov and A. B. Shabat, "Exact theory of two dimensional self-focusing and one dimensional self-modulation of waves in nonlinear media," *Sov. Phys. JETP*, vol. 34, pp. 62–69, 1972.
[34] A. Hasegawa and Y. Kodama, *Solitons in Optical Communications*. Oxford, U.K.: Oxford Univ. Press, 1995.
[35] J. P. Gordon and H. A. Haus, "Random walk of coherently amplified solitons in optical fiber transmission," *Opt. Lett.*, vol. 11, pp. 665–667, Oct. 1986.
[36] D. Marcuse, "An alternative derivation of the Gordon-Haus effect," *J. Lightwave Technol.*, vol. 10, pp. 273–278, Feb. 1992.
[37] K. Tamura and M. Nakazawa, "Timing jitter of solitons compressed in dispersion decreasing fibers," *Opt. Lett.*, vol. 23, pp. 1360–1362, Sept. 1998.
[38] M. Nakazawa, E. Yoshida, and Y. Kimura, "Ultrastable harmonically and regeneratively mode-locked polarization maintaining erbium fiber ring laser," *Electron. Lett.*, vol. 30, pp. 1603–1605, Sept. 1994.
[39] M. Nakazawa, E. Yoshida, K. Kubota, and Y. Kimura, "Generation of a 170 fs, 10 GHz transform-limited pulse train at 1.55 μm using a dispersion-decreasing, erbium-doped active soliton compressor," *Electron. Lett.*, vol. 30, pp. 2038–2040, Nov. 1994.
[40] T. Miya, K. Okamoto, Y. Ohmori, and Y. Sasaki, "Fibrication of low dispersion single mode fibers over a wide spectral range," *IEEE J. Quantum Electron.*, vol. QE-17, p. 858, 1981.
[41] K. R. Tamura and M. Nakazawa, "Femtosecond pulse generation over a 32 nm wave-length range using a dispersion-flattened dispersion-decreasing fiber," *IEEE Photon. Technol. Lett.*, vol. 11, pp. 319–321, Mar. 1999.
[42] T. Komukai, K. Tamura, and M. Nakazawa, "An efficient 0.04-nm apodized fiber Bragg grating and its application to narrow-band spectral filtering," *IEEE Photon. Technol. Lett.*, vol. 9, pp. 934–936, July 1997.

Kohichi R. Tamura (M'95), photograph and biography not available at the time of publication.

Hirokazu Kubota, photograph and biography not available at the time of publication.

Masataka Nakazawa (M'84–SM'92–F'95), photograph and biography not available at the time of publication.